Chapter 3

Green synthesis of TiO_2 nanoparticles using *Tinospora cordifolia* plant extract & its potential application for photocatalysis and antibacterial activity

Abstract

Green synthesis is a straightforward, non-toxic, cost-effective, and eco-friendly method of synthesizing nanoparticles. The present study used *Tinospora cordifolia* plant stem extract to synthesize Titanium (IV) dioxide nanoparticles (TiO_2 NPs). The plant extract was characterized using Fourier transform infrared spectroscopy (FTIR). Obtained NPs were characterized using scanning electron microscopy (SEM), FTIR, and X-ray diffraction (XRD). The XRD pattern demonstrated the anatase phase formation and the existence of nano-crystalline TiO_2 with an average crystallite size of 15.02 nm. The optical characteristics of NPs were identified by UV-visible spectroscopy. SEM study revealed that the synthesized nanoparticle was triangular-shaped and the synthesized NPs' average size was in the nanometers range. The optical energy band gap of synthesized TiO_2 was 3.13 eV. The average hydrodynamic radius and zeta potential of synthesized TiO_2 NPs were 153.4 nm and -28.4 mV, respectively. Acid Blue 113 was photo-catalytically degraded through green synthesized TiO_2 NPs. Under optimum operating conditions, 94.43% AB 113 degradation occurred in 80 minutes. The degradation reaction follows pseudo-first-order reaction kinetics having a reaction rate constant value of 0.03362 min^{-1}. The zone of inhibition exhibited by TiO_2 NPs was 13 ± 0.39 and 26.5 ± 0.79 mm corresponding concentrations of 150 and 500 µg/mL, respectively.

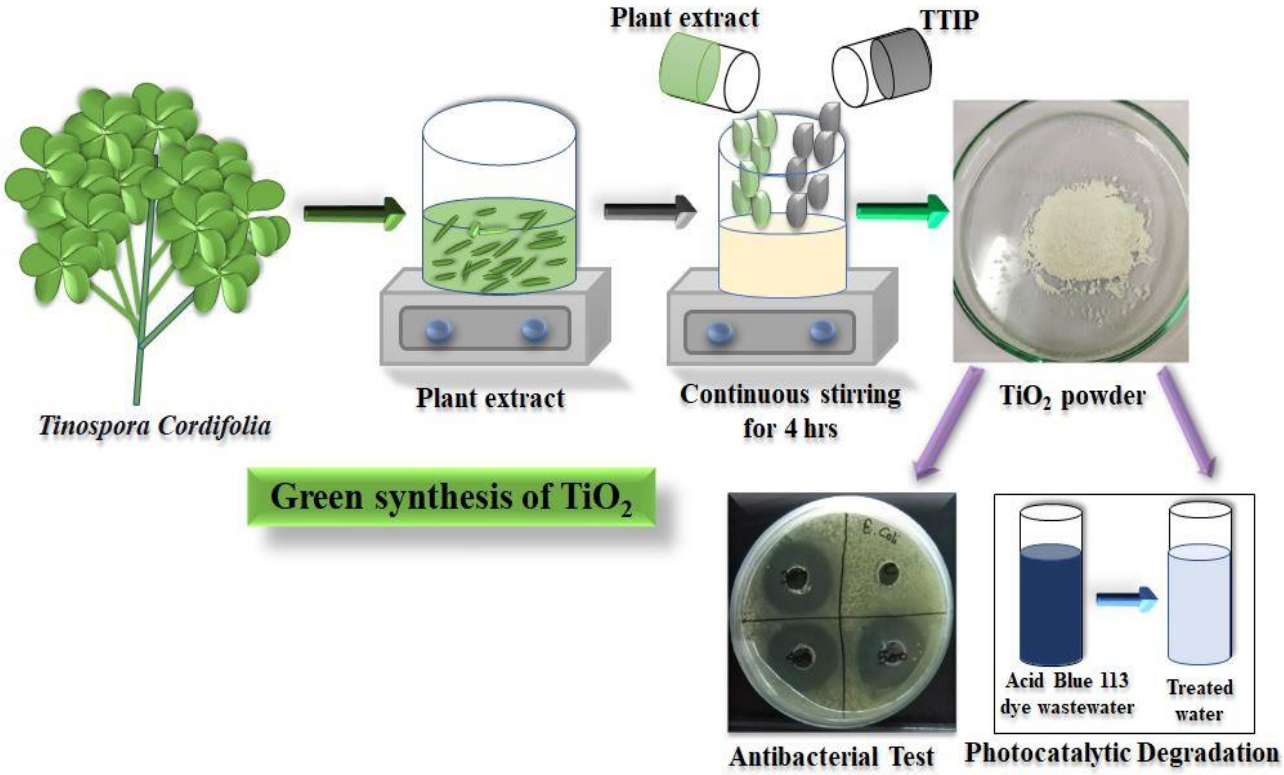
Plant extract
TTIP
Tinospora Cordifolia
Plant extract
Continuous stirring for 4 hrs
TiO2 powder
Green synthesis of TiO2
Antibacterial Test
Acid Blue 113 dye wastewater
Treated water
Photocatalytic Degradation

3.1 Introduction

An important worldwide issue right now is protecting the environment. Several strategies for treating organic contaminants in wastewater have been documented in the previous few decades [81–83]. Many researchers are interested in the photocatalysis of metal nanoparticles [84]. Because of the enormous surface area and ease of removal from the reaction mixture, nano-catalysis has gained popularity as a reusable catalyst. The magnetic, electrical, and optical characteristics of metal oxide nanoparticles are diverse [85]. The present era of ecologically friendly metal/metal-oxide nanoparticle (NPs) synthesis, sometimes known as "green synthesis," has gotten a lot of attention for its potential uses in water pollution, painting, and nanotechnology. The plant (leaves, stem, flower, and root) extract contains components that cause metal ions to be reduced. It also possesses natural and effective capping agents in the form of proteins to keep NPs stable [86].

TiO_2 NPs are n-type semiconductors with a white hue that have drawn attention because of their various applications across many sectors [87,88]. There are three phases of TiO_2: rutile, anatase, and brookite [89]. The rutile phase is the most stable among the three phases, whereas the subsequent two phases can be converted to the rutile phase by heating. The anatase and rutile phase exist in tetragonal crystalline forms, while the brookite phase exists in the orthorhombic crystalline form [90]. Because of its large surface area, high potential energy for photogenerated charge carriers, and superior photocatalytic activity, anatase is the preferred form [91]. Under ultraviolet (UV) light, Fujishima and Honda discovered the phenomena of photocatalytic water splitting on a TiO_2 electrode in 1972. It has progressed since then in the areas of photovoltaics, photo/electrochromic, sensors, and photocatalytic applications for the elimination of various organic pollutants from water [92]. Because of its high stability, low cost, and safety for both humans and the environment, TiO_2 is considered a near-ideal semiconductor for photocatalysis. It has a high refractive index, high adsorption and

photocatalytic capacity towards specific pollutants, high binding affinity, and oxygen vacancies in the lattice structure [30]. TiO_2 nanoparticles have been manufactured by a variety of methods, including physical, chemical, and green synthesis, which are discussed in Chapter 1. The green route for the synthesis of TiO_2 can be an effective method for TiO_2 NPs synthesis.

Based on the author's knowledge, limited efforts have been carried out for the synthesis of TiO_2 nanoparticles utilizing *Tinospora cordifolia* plant extract. *Tinospora cordifolia*, also known as "*Guduchi*" in Sanskrit, is a member of the *Menispermaceae* family. It is a deciduous climbing shrub with greenish-yellow blooms that bloom at higher altitudes and is genetically varied. The key advantages of TiO_2 NPs are comprised of high stability, low cost, non-toxic, and safe for both humans and the environment [93]. Alkaloids, diterpenoid lactones, glycosides, steroids, sesquiterpenoids, phenolics, aliphatic chemicals, and polysaccharides are the most common constituents [94]. *T. cordifolia* plant extract is widely employed in anti-periodic, anti-spasmodic, anti-microbial, anti-osteoporotic, anti-inflammatory, anti-arthritic, anti-allergic, and anti-diabetic herbal medicines [95].

Large volumes of recalcitrant organic effluents are released into the aquatic environment from numerous industries such as dyeing, food, leather, medicines, petroleum, textiles, pulp, paper, sugar, and plastic manufacturing. These pollutants severely lead the water pollution, deplete the dissolved oxygen level, and also deteriorate aquatic life by directly affecting their respiratory cycle. Among these polluting sources, the textile industry generates around 17–20 percent of total industrial effluents [96]. The major consequences of textile effluents mostly containing various dyes are discussed in Chapter 1. The photocatalytic oxidation technique is one of the most popular techniques, having a widespread application for organic pollutant degradation, which is also discussed in Chapter 1.

The present study incorporated the potential application of green synthesized TiO_2 NPs for the effective mineralization of a typical complex Acid Blue 113 (AB113) dye. Because of the azo

groups (-N=N-), AB113 dye has poor biodegradability and degrades slowly. The International Agency for Research on Cancer (IARC) has categorized AB113 as a potential carcinogenic [97]. Green synthesized TiO_2 NPs' antibacterial activity has also been elucidated. Various process aspects including the effect of various parameters such as dye concentration, pH, and catalyst dose have also been examined.

3.2 Materials & methods

3.2.1 Materials

Titanium (IV) isopropoxide (TTIP, Ti $[OCH(CH_3)_2]_4$, CAS number: 546-68-9; MW: 284.22; purity >97%), used as a precursor for Titanium (IV) oxide (TiO_2), purchased from Sigma Aldrich. Acid Blue 113 ($C_{32}H_{21}N_5Na_2O_6S_2$; CAS number: 3351-05-1; MW: 681.65) dye was purchased from Sigma Aldrich. All the chemicals used in the present finding were of high purity analytical grade and used without any further purification. **Fig. 3.1** shows the molecular structure of AB 113 dye.

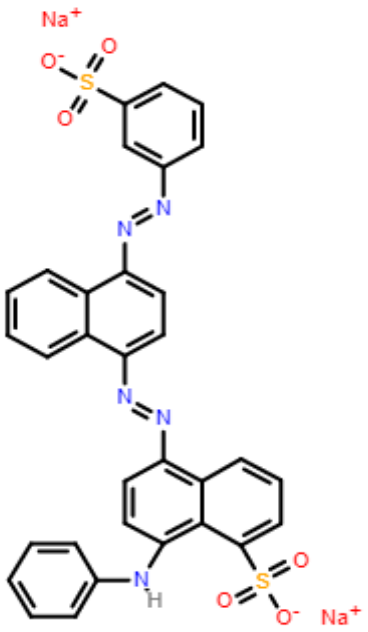

Fig. 3. 1 Molecular structure of Acid blue 113 dye.

3.2.2 Preparation of Plant Extract

The stem of the *Tinospora cordifolia* plant vine, collected from the campus of IIT BHU, was washed with double distilled water to remove any debris stuck to the surface and remove the outer layer. Cut these samples into 0.5 to 1 cm pieces, thereafter into the 4-5 pieces axially. Weigh 15 g of plant stem and feed it into an Erlenmeyer flask (250 mL) containing 100 mL of distilled water. The entire mixture was heated and mixed in a magnetic stirrer for 3 h at 90°C and 650 rpm. At the end of 3 h, the color of the resulting mixture was changed from green to olive green. Filtration was used to separate solid biomass and the plant extract was then recovered and stored inside a refrigerator to maintain the temperature between 0 to 5°C until future usage.

3.2.3 Green synthesis of TiO_2 NPs

In an Erlenmeyer flask, mix 20 mL TTIP with 20 mL plant extract in a 1:1(v/v) ratio at 50°C with continuous stirring (600 rpm) using a magnetic stirrer. After 4 h, the color of the solution changed from white to light yellow, indicating a decrease in Titanium ions (Ti^{+4}) concentration. Vacuum filtration was employed to separate the precipitates from the resulting mixture and ethanol was used to eliminate ionic and other contaminants. In an electric oven, the washed precipitates were dried. The obtained dry samples were pulverized into a fine powder with a mortar pestle. In a muffle furnace, fine TiO_2 powder was obtained and calcined at 400°C (**Fig. 3.2**). Flavonoids, terpenoids, and phenolic acids are naturally occurring organic compounds present in plant extract of *Tinospora cordifolia* and act as reducing and stabilizing agent for the synthesis of TiO_2 nanoparticles, these compounds stabilize the nanoparticles to avoid aggregation and also reduce the precursor to TiO_2 nanoparticles.

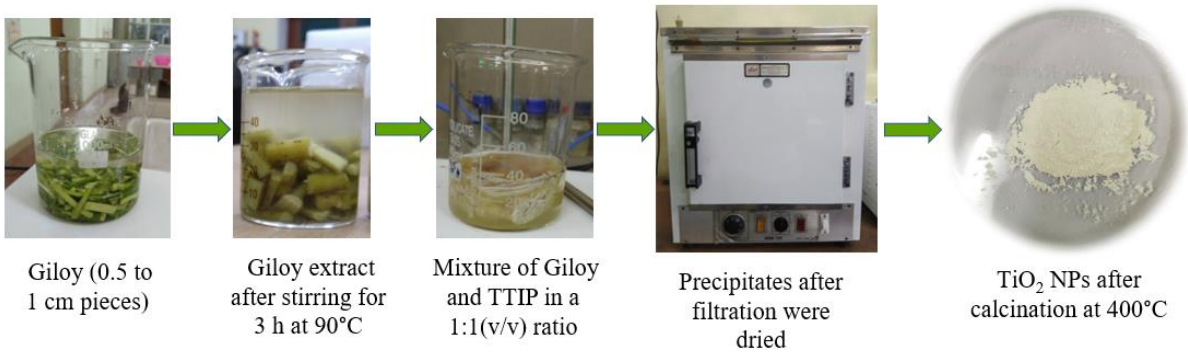

Fig. 3. 2 A typical illustration of green synthesis of TiO_2 NPs from *Tinospora cordifolia* (Giloy).

3.2.4 Characterization of Green synthesized TiO_2 NPs

A zeta potential analyzer was used to examine the particle size distribution of anatase TiO_2 NPs, their stability in colloidal solution, and zeta potential distribution (Malvern Panalytical, Zetasizer Ver. 7.13, Serial Number: MAL1213575). The UV-Vis spectrophotometer (SL-159, Elico, India) was used for the measurement of absorbance spectra of the AB 113 oxidized samples as also the TiO_2 NPs, moreover, Tauc's plot was used to calculate their band-gap energy (E_g). The structural features of TiO_2 NPs, such as phase evolution, crystallite size, and inter-planar spacing between crystallographic planes, were determined using High-resolution X-ray diffraction (HR-XRD) (Rigaku SmartLab 9kW Powder type, RIGAKU Corporation). A Cu-Kα radiation source (λ = 1.5406 nm) was used with an accelerating voltage of 30 kV and an electronic current of 30 mA in the XRD apparatus. The diffraction patterns were obtained within the range of 10°–80°. Scanning Electron Microscope (MA15/18, Carl Zeiss Microscopy Ltd.) images revealed the surface morphology of the green synthesized TiO_2 NPs. BET surface area analysis was conducted on a MicrotracBEL instrument with a soaking time of 6 h and a target temperature of 200°C at a rate of 5°C/min.

The Fourier-transform infrared spectra (FTIR) (Nicolet iS5, THERMO) analysis was used to identify the various functional groups present on the surface of the TiO_2 sample as well as in the *Tinospora cordifolia*. The sample was pre-mixed in a 5:95 ratio with spectroscopically pure

KBr [98,99]. The spectra were taken using an FTIR spectrophotometer in the mid-infrared range of 4000-500 cm^{-1} at 32 scan speed and 4 cm^{-1} resolution.

3.2.5 Photocatalytic degradation of Acid Blue 113 dye

The photocatalytic oxidation of AB 113 dye was carried out in a photocatalytic reactor (4 cm ID and 60 cm height). The plexiglass cylinder was irradiated with a UV source (125 W). The wavelength of the photocatalytic degradation of AB dye using TiO_2 as the catalyst is in the UV range, with a wavelength of 288 nm. The photocatalytically oxidized AB 113 dye samples were withdrawn at regular time intervals and centrifuged at 4500 rpm for 15 min (REMI CENTRIFUGE, RM-12C BL). Subsequently, the dye solution was filtered using a syringe filter (0.44 μm) and the absorbance of the clear supernatant was measured (λ_{max} = 550 nm) to assess the photocatalytic performance. The percentage removal of dye was calculated using the following equation [100]:

$$\% \text{ Removal of AB113 dye} = \frac{OD_0 - OD_t}{OD_0} \times 100 \quad (4)$$

where, OD_0 and OD_t are abbreviated for the absorbance of AB 113 at an initial stage and after the photocatalytic oxidation, respectively.

3.2.6 Antibacterial activity of TiO_2 NPs using agar well diffusion method

The antibacterial activity of TiO_2 NPs against *Escherichia coli* (*E. coli*) was investigated by the agar well-diffusion method. Briefly, the sterile molten Nutrient agar media was poured into Petri dishes and allowed to solidify at room temperature. A well-grown culture of *E. coli* was uniformly spread into the petri dish. Wells were cut in the plates using a sterile cork-borer and 150, 200, 250, 300, 400, and 500 μg/mL of TiO_2 solution were dispensed into each well. The agar well diffusion test was examined at the end of 24 h of incubation duration (30 ± 5°C) under dark conditions [101]. After 24 h of incubation, the zone of inhibition was measured based on *E. coli* culture-free circular diameter.

3.2.7 Statistical analysis

Triplicate analyses of each experiment were carried out. The Tukey-Kramer multiple comparison test and one-way analysis of variance with a p-value ($p \leq 0.05$) were used to analyze the data.

3.3. Results & Discussion

3.3.1 X-ray diffraction

The crystalline nature of TiO_2 NPs was elucidated using XRD spectra (**Fig. 3.3**). The diffraction peaks were seen at 25.33°, 37.90°, 47.89°, 53.90°, 54.94°, 62.74°, 70.18°, and 74.96°, corresponding Miller indices were found to be (101), (004), (200), (105), (211), (204), (220) and (215), respectively according to JCPDS (file No. 021-1272). The (hkl) values of the indexed peaks were matched with the standard (hkl) values of anatase TiO_2 NPs quite well. The pattern had shown no extra impurity peaks, indicating that TiO_2 was in its pure anatase phase (**Fig. 3.3**). The sharp and broad diffraction peaks reflected the crystallinity and nano-sized crystallite composition of the particles, respectively. Since just a small number of atoms in the nanoparticles were involved in the diffraction, the peaks seemed wider. These atoms dispersed because they were unable to form a straight diffraction line. Using Scherer's equation (Eq.1), the average crystallite size of TiO_2 NPs was estimated from the XRD pattern [102].

$$D = \frac{k\lambda}{\beta \cos\theta} \quad (1)$$

where D: is the NPs' crystalline size, λ: represents the X-ray radiation source's wavelength, k = 0.89: is a constant crystalline shape factor, θ: The Bragg's diffraction angle, and β: is the full angular width at half maximum (FWHM) in radian of XRD peaks recorded at diffraction angle 2θ. Green synthesized TiO_2 NPs' average crystallite size was found to be 15.02 nm and the key findings were illustrated in **Table 3.1**. The average particle size was also calculated and it was found to be 25.21 nm.

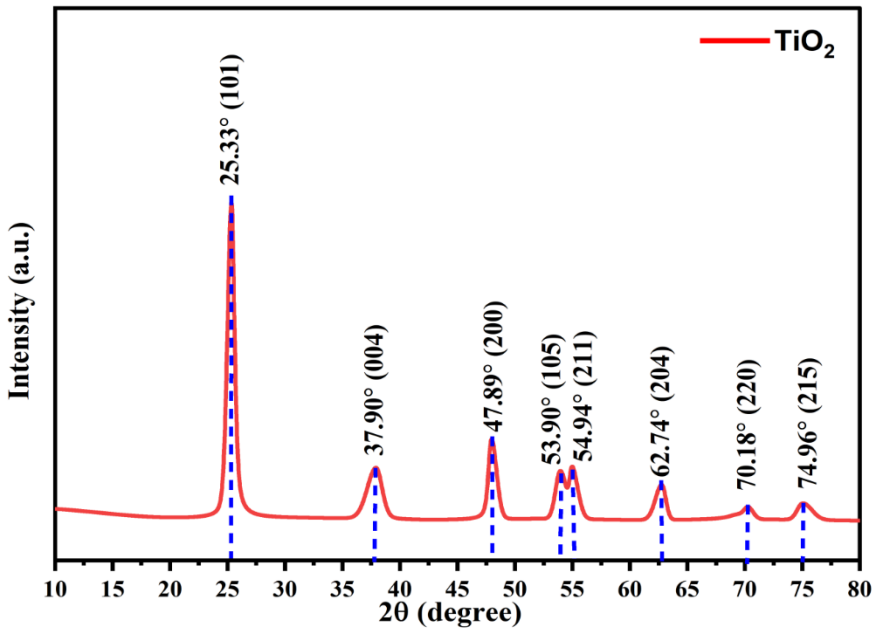

Fig. 3. 3 Typical XRD spectra of green synthesized TiO_2 NPs.

Table 3. 1 XRD key findings of green synthesized TiO_2 NPs.

S.N.	Peak position 2θ (degree)	Peak width FWHM (Degree)	Lattice Planes (hkl)	Inter planer distance (nm)	Crystalline size D (nm)
1	25.33	0.73	101	3.514	11.90
2	37.90	1.51	004	2.372	6.60
3	47.89	0.81	200	1.8978	14.46
4	53.90	1.10	105	1.700	12.12
5	54.94	0.83	211	1.6699	16.47
6	62.74	1.03	204	1.4798	16.65
7	70.18	1.1	220	1.340	21.06
8	74.96	1.45	215	1.2659	20.87
					D_{avg} =15.02

3.3.2 UV-Vis spectrophotometer analysis and computation of energy band gap (E_g) of TiO_2 NPs

The UV-Vis absorbance spectral profile (λ_{max} = 288 nm) of green synthesized TiO_2 NPs was illustrated in **Fig. 3.4**. Tauc's equation (Eq. 2) and the absorbance spectrum of TiO_2 were used for the computation of the energy band gap of TiO_2 NPs [103].

$$(\alpha h\nu) = A\left(h\nu - E_g\right)^n \quad (2)$$

where α abbreviates for absorption coefficient, h is Plank constant (6.626×10^{-34} J.s), ν represents the frequency of incident light, A is constant, E_g denotes the optical energy band gap of the semiconductor TiO_2 and n is a constant (depending on the transition characteristics, it may have values of $\frac{1}{2}$, 2, $\frac{3}{2}$ and 3 which correspond to allowed direct, allowed indirect, forbidden direct, and forbidden indirect transitions, respectively). The E_g (3.13 eV) was obtained by extrapolating the linear portion of the curve to the X-axis (hν) (**Fig. 3.5**). The above findings indicated that the E_g value of green synthesized TiO_2 was lower than that of standard anatase TiO_2 (3.2 eV). The low E_g was reasonably in the favor of high photocatalytic activity of synthesized TiO_2 NPs. As a result, the energy consumption during UV irradiation diminished. A similar study was carried out for the synthesis of TiO_2 using *Acorus calamus* leaf extract and reported the band gap energy to be 3.20 eV [104]. Another study reported a band gap energy of 3.25 eV for synthesized TiO_2 NPs [105]. Thus, it can be concluded that the green synthesis of TiO_2 NPs remarkably diminished the band gap energy and alleviated the photocatalytic activity.

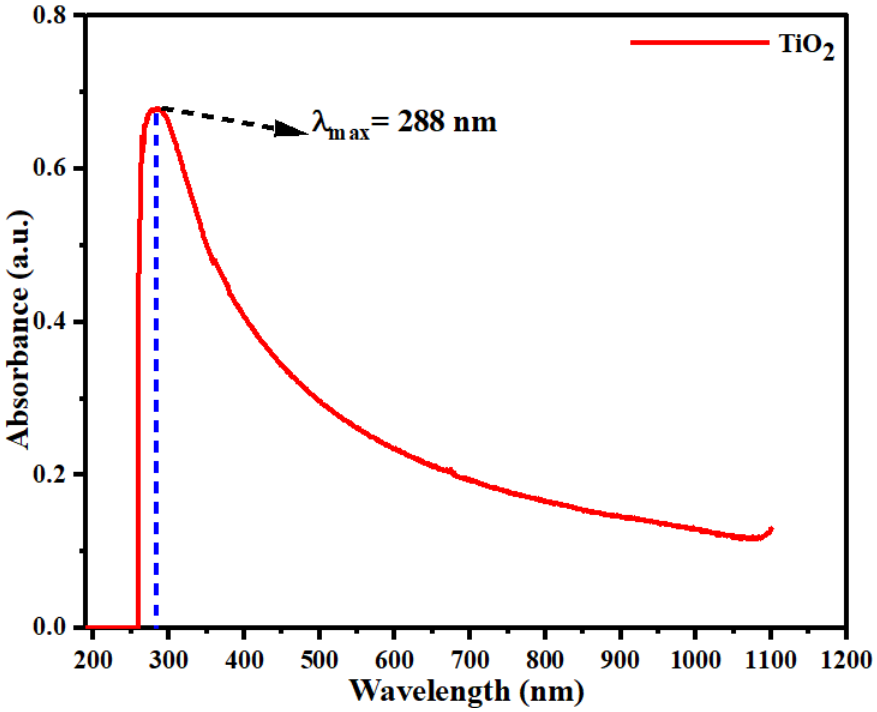

Fig. 3. 4 An illustration of the UV-Vis absorbance spectrum of green synthesized TiO_2 NPs.

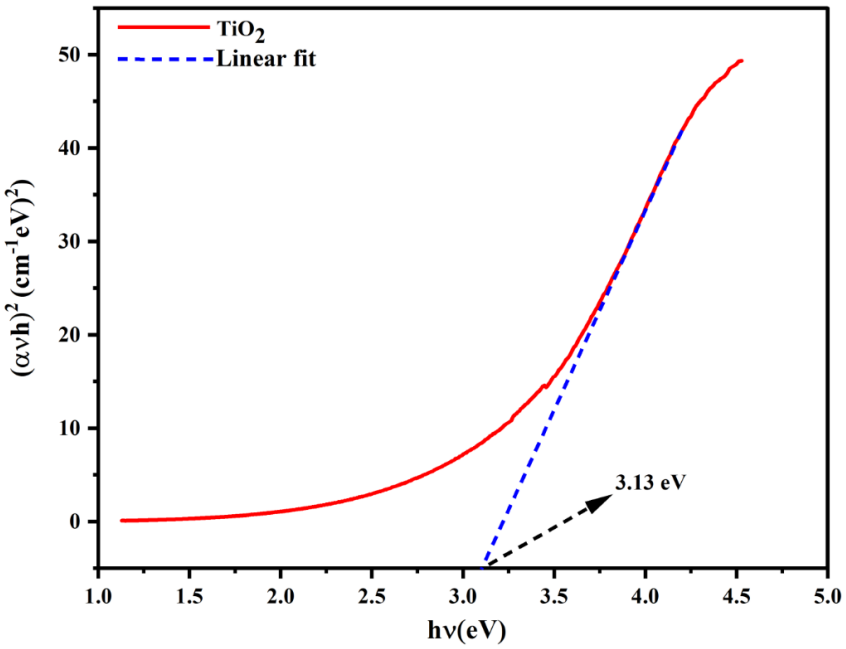

Fig. 3. 5 An illustration of Tauc's plot for the green synthesized TiO_2 NPs used for the calculation of their energy band gap through linear extrapolation.

3.3.3 Brunauer-Emmett-Teller (BET) surface area

The textural properties of Green synthesized TiO_2 NPs were determined by using the BET surface area measurement. Based on the experimental findings, the BET surface area of green synthesized TiO_2 was determined to be 60.8 m^2/g (**Fig. 3.6a**) and reasonably facilitated enough contact area for the dye molecule to adsorb and oxidize. The average pore diameter and mean pore volume of TiO_2 NPs were determined to be 13.827 nm and 0.1881 cm^3/g, respectively. The N_2-adsorption/desorption isotherms of the TiO_2 are depicted in **Fig. 3.6(b)**. The BJH pore size distribution curve of TiO_2 from the adsorption branch was shown in **Fig. 3.6(c)** indicating their mesopores structure. The isotherm of the TiO_2 catalyst was found to be type IV with a hysteresis loop type H2 supporting good connectivity between the pores and numerous mesopores in the bulk phase of green synthesized TiO_2 according to the IUPAC classification [106].

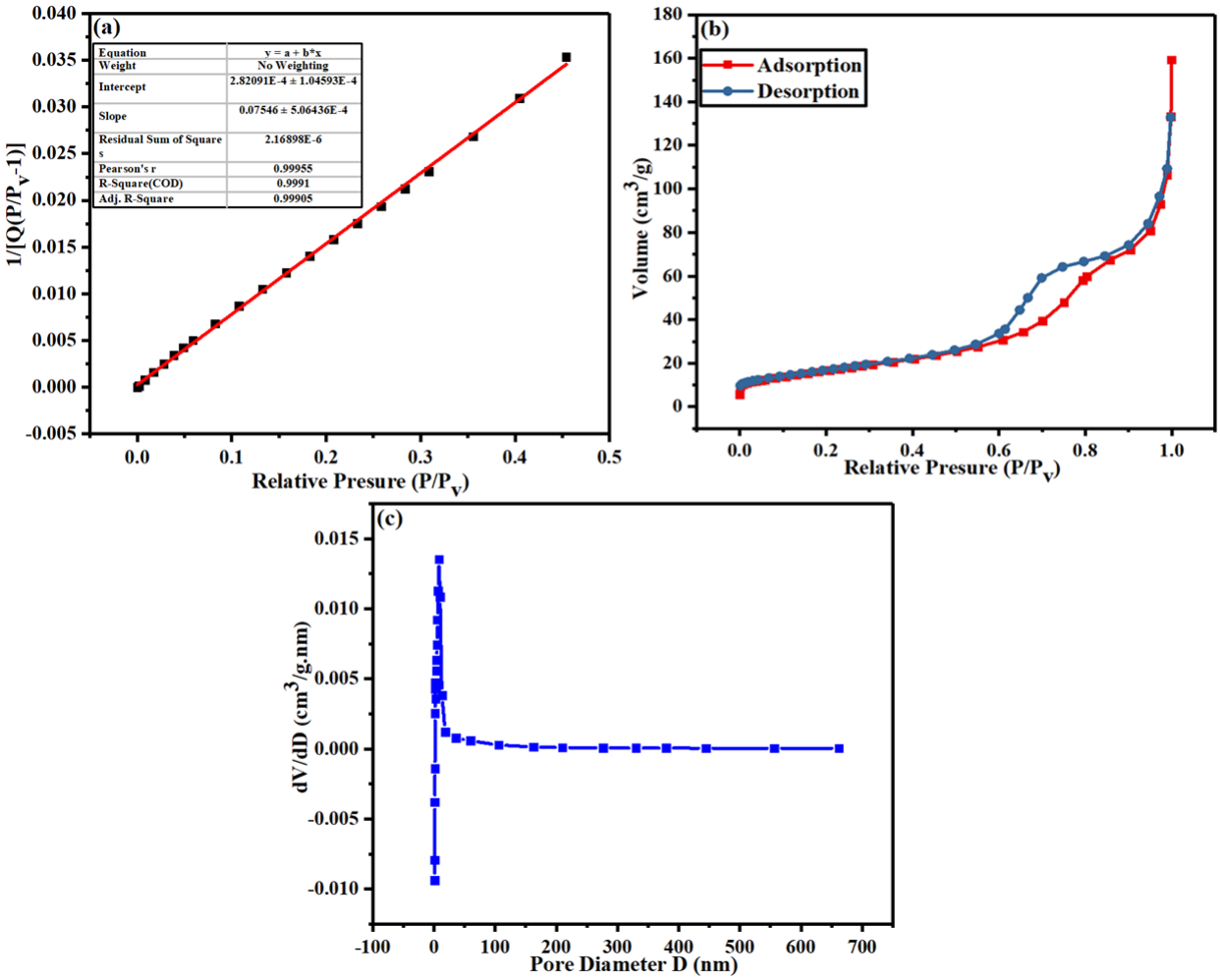

Fig. 3. 6 (a) BET surface area analysis of green synthesized TiO_2 NPs. (b) Hysteresis loops in N_2 adsorption/desorption isotherms for TiO_2 NPs. (c) Barrett-Joyner-Halenda (BJH) pore size distribution of TiO_2 NPs.

3.3.4 FTIR spectral analysis

The FTIR spectral analysis of *T. Cordifolia* showed the major peaks 3332 cm^{-1} (O-H stretching alcohol), 1637 cm^{-1} (C-O stretch, carbonyl group; C-H stretch) and 660 cm^{-1} (-OH, hydroxyl group) **(Fig. 7a)** [107].

The chemical structure of green synthesized TiO_2 NPs was examined using FTIR spectroscopy to validate whether they have the presence of corresponding functional groups (**Fig. 7b**). Several major peaks appeared in the FTIR spectrum at 3455, 2964, 1468, 1094, and 791 cm^{-1}, respectively. The characteristic peak at 791 cm^{-1} is attributed to the Ti-O stretching of the

anatase phase of TiO_2 [108]. The Ti-O stretching and Ti-O-Ti bridging stretching modes were attributed to broadband from 1000 to 500 cm^{-1} [109]. Around 3455 cm^{-1}, a spectroscopic band was found, leading to the presence of both symmetric and asymmetric stretching vibrations of the hydroxyl group (Ti–OH) [110]. The characteristic frequency of leftover organic species, which was not eliminated by ethanol and distilled water washing, was assigned to C-H stretching vibrations of alkane groups, resulting in a peak at 2964 cm^{-1} [111]. Bending vibrations of H–O–H of chemisorbed water molecules are responsible for the peak at 1468 cm^{-1} [86].

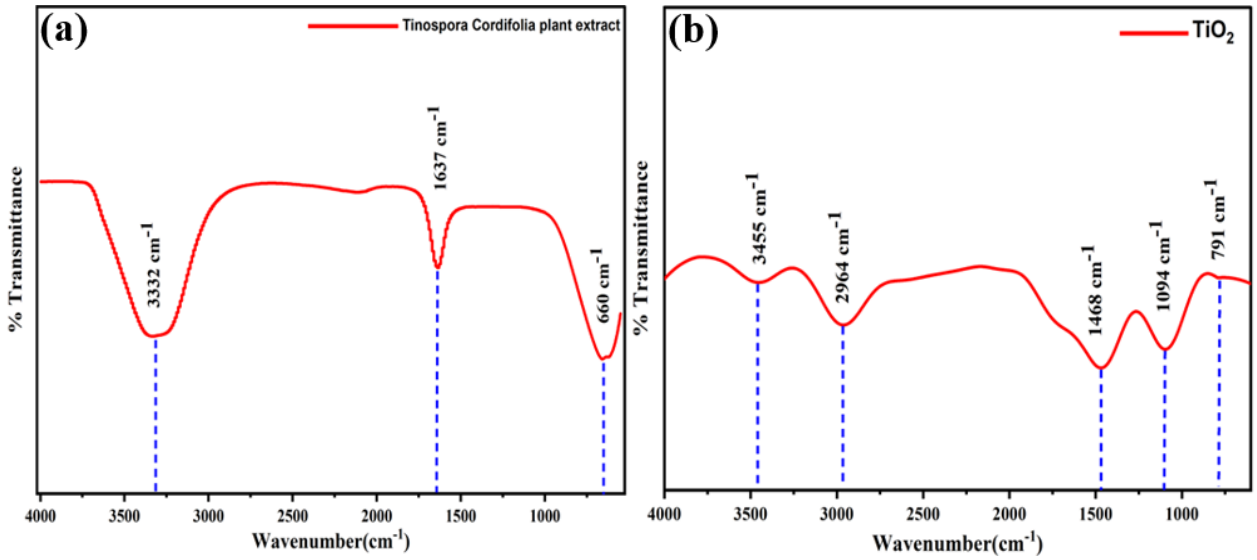

Fig. 3. 7 (a) The FTIR Spectral profile of *Tinospora cordifolia* plant extract and (b) An illustration of the FTIR spectral profile of green synthesized TiO_2 NPs from *Tinospora cordifolia* plant extract.

3.3.5 Zeta Potential and Particle Size Distribution of TiO_2 NPs

The green synthesized anatase TiO_2 NPs were approximately mono-disperse in nature, having an average hydrodynamic radius of 153.4 nm (**Fig. 3.8a**). The zeta potential i.e., the net surface charge of -28.4 mV revealed that the anatase TiO_2 formed a stable colloidal solution (**Fig. 3.8b**).

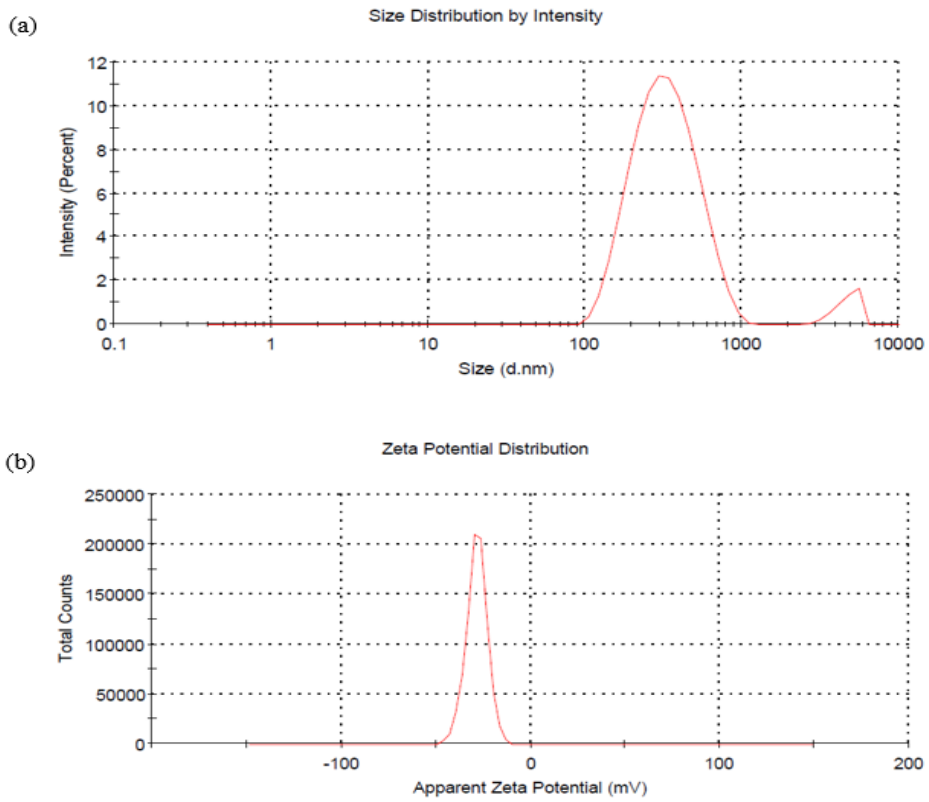

Fig. 3. 8 (a) A typical illustration of the distribution of TiO_2 NPs and (b) the distribution of surface potential i.e., (Zeta Potential) based on intensity and total counts, respectively.

3.3.6 SEM analysis

Scanning electron microscopy of green synthesized TiO_2 NPs at various magnifications, revealed an irregular and angular nanostructure with a dense porous network, as well as the reduction of NPs aggregation by *Tinospora cordifolia* plant extract, which was used as a capping and reducing agent (**Fig. 3.9**). It could be observed that all the particles were at the nano-range. When compared to the rod and spherical-shaped NPs, the morphology of triangular and irregularly shaped TiO_2 NPs enhanced antibacterial and anticancer activity [87,112]. The plant extract was used to achieve non-aggregation and good dispersibility of NPs, which is consistent with our findings [113]. The green synthesis facilitates the usefulness of TiO_2 NPs for several biological applications [114]. The TEM analysis, from the magnification of the TEM image, confirms that all the particles were at the nano-range. and morphology is observed

to be irregular and agglomerated in some areas. The bright rings in the SAED pattern are related to the standard polycrystalline rings of diffraction of the anatase phase **(Fig. 3.9(f))**.

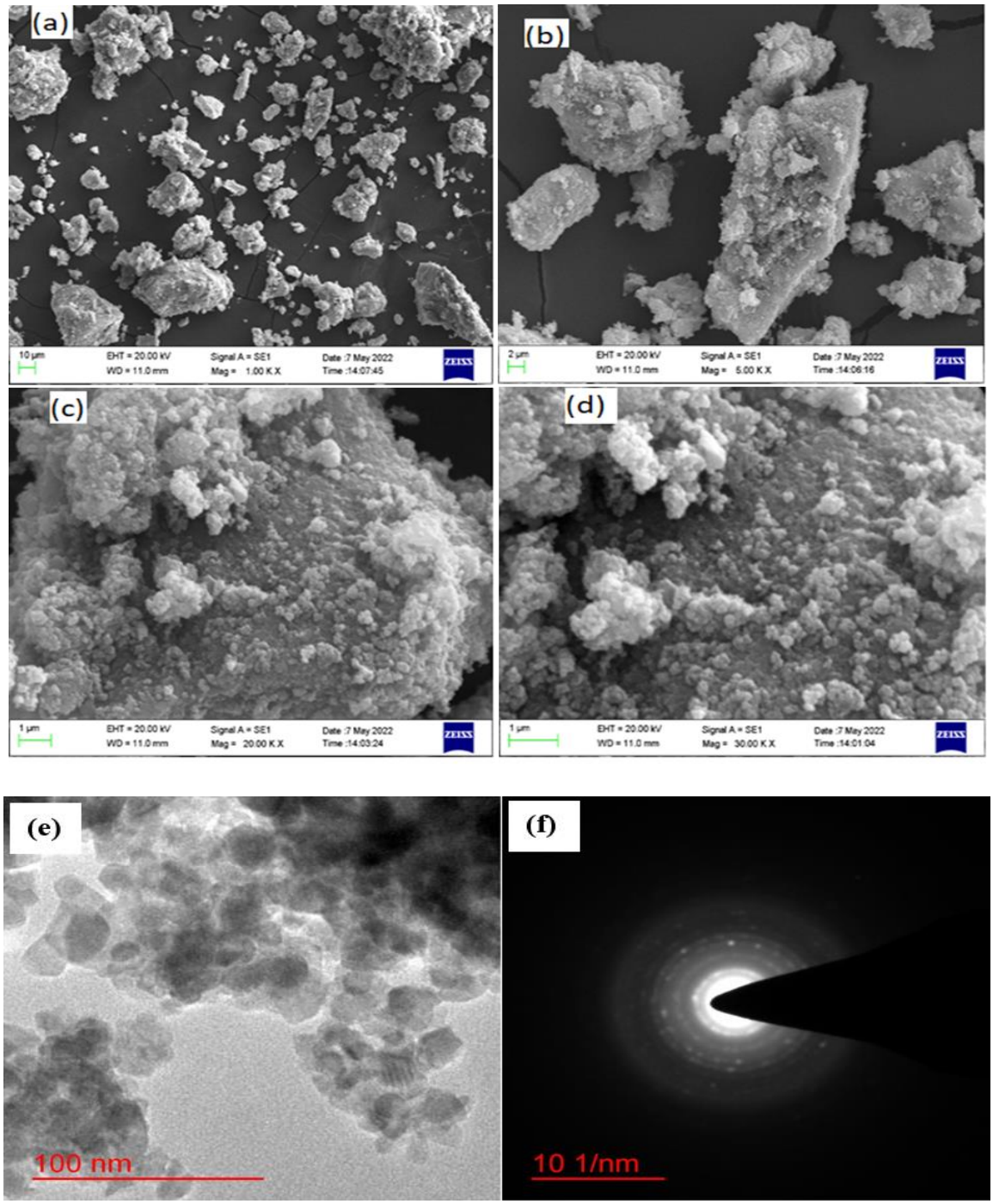

Fig. 3. 9 SEM micrographs of green synthesized TiO_2 NPs at different magnifications (a) ×1K times (b) ×5K times (c) ×20K times and (d) ×30K times (e) TEM image of green synthesized TiO_2 (f) and SAED pattern.

3.3.7 Photocatalytic activity of the synthesized photocatalyst

In order to validate the photocatalytic activity of green synthesized TiO_2 NPs, a preliminary study was carried out to investigate the effect of different parameters on the removal efficiency of a complex AB 113 dye. The exposure of NPs under UV irradiation merely enhanced the decolorization of the dye. The degradation process has begun as UV irradiation leads to photoexcitation. The UV-Vis absorbance spectral profile depicted that the maximum absorbance was obtained corresponding to the wavelength of 550 nm (**Fig. 3.10a**), therefore all the absorbance of photocatalytic oxidized products was computed corresponding to this wavelength.

3.3.7.1 Effect of initial catalyst dosage

TiO_2 NPs had significantly high catalytic activity since the band gap energy was reduced. The amount and size of the photocatalyst directly affected the photocatalytic oxidation of AB 113. The available active surface area of the photocatalyst was increased and is liable for more removal efficiency of AB 113. The active sites available for UV irradiation and the generation of e^-/h^+ pair and reactive oxidation species (ROS) (i.e., OH•) depend on their amount [81]. As the catalyst dose increased to 2.0 g/L, a maximum of 85.42% removal efficiency of AB 113 was obtained (**Fig. 3.10b**). This fact could be attributed to the fact that as the catalyst loading enhanced the generation of ROS also surged and facilitated the mineralization of AB 113. The active sites were also significantly enhanced and directly alleviated the photocatalytic activity of TiO_2. As the loading was further increased to 2.5 g/L, the removal efficiency declined to 75.78%. This could be because the solution became more opaque as the catalyst amount was further increased, as a result, the attenuation of UV irradiation intensity occurred. Therefore, the generation of OH• decreased as also the agglomeration of TiO_2 particles took place [115]. This finding indicates that the TiO_2 NPs synthesized using plant extract are effective in removing organic pollutants from wastewater, which is a significant environmental issue.

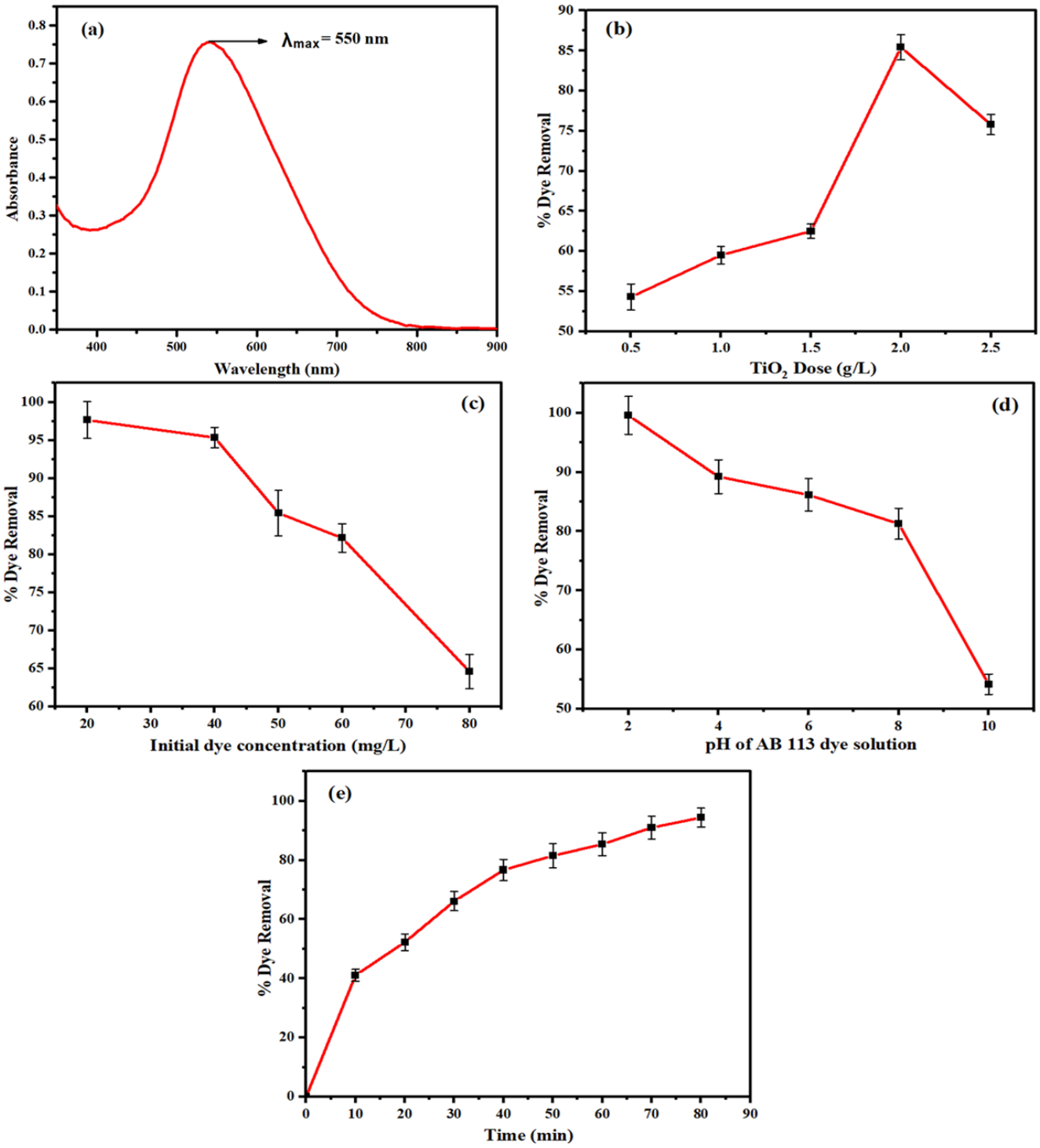

Fig. 3. 10 (a) UV-Vis absorbance spectrum of Acid Blue 113 (λ_{max} = 550 nm); (b) Effect of TiO_2 dose on dye removal; (c) Effect of initial dye concentration on AB 113 removal; (d) Effect of pH on dye removal efficiency; (e) Effect of UV irradiation duration on AB 113 removal (Error bars indicated the standard deviation of triplicate study).

3.3.7.2 Effect of initial dye concentration

AB 113 dye concentration was varied from 20 to 80 mg/L and examined the dye removal efficiency. However, the irradiation intensity remained constant, and an optimum catalyst amount of 2 g/L was used for carrying out the photocatalytic oxidation study. The removal efficiency steadily decreased from 97.64 to 64.6% as the dye concentration varied from 20 to 80 mg/L, respectively. A higher concentration of AB 113 somehow reduced the photon adsorption frequency and resulted in a reduction in dye removal efficiency (**Fig. 3.10c**). This was most likely since raising the dye concentration while keeping the catalyst dose constant allowed the fixed number of catalysis sites to be saturated faster. Furthermore, higher dye concentrations were likely to reduce the penetration of light in the solution. Reduced UV penetration can limit TiO_2 particle activation rates and obstruct the production of •OH radicals, resulting in lower photocatalytic oxidation efficiencies [116].

3.3.7.3 Effect of pH

Surface charge and electrostatic interaction between the catalyst and organic pollutant is one of the crucial factors governing their interaction. The pH of the solution was varied from 2 to 10 and examined the dye removal performance (**Fig. 3.10d**). AB 113 removal efficiency declined as the solution pH altered from an acidic medium to an alkaline medium. The above finding was attributed due to the presence of more hydroxyl ions, which were liable to prevent the dye molecule interaction with the active sites of the photocatalyst [81]. Anatase TiO_2 exhibited a point of zero charges (PZC) at 6.1, therefore the surface charge was positive at pH lower than 6.1 whereas it remained negative above it. AB 113 structure revealed the presence of two sulfonate groups (SO_3^-) which also remained negatively charged. Therefore, the acidic medium is liable for more electrostatic attraction between the dye and catalyst surface as compared with the alkaline medium. Thus, a maximum dye removal efficiency was obtained at lower pH values.

3.3.7.4 Effect of reaction time

The residence time of UV irradiation and complex AB 113 on the active sites of anatase TiO_2 reasonably enhanced the oxidation of AB 113. As the contacting time increased the dye removal efficiency also steadily increased. Therefore, for an 80-minute irradiation duration, a maximum of 94.43% dye removal was obtained and it was below the permissible limit of the concentration of AB 113 dye in textile effluent as per the Indian government guidelines [117,118]. After an 80 min irradiation duration, further oxidation of AB 113 diminished (**Fig. 10e**). The above findings were obtained at the dye concentration of 50 mg/L, pH 4, and an amount of anatase TiO_2 was 2 g/L. The generation of OH• was responsible for more dye removal efficiency. A comparative analysis of our findings with available literature was elucidated in **Table 3.2**.

Table 3. 2 A comparative study of dye removal using synthesized TiO_2 based on available literature.

S.N.	Dye Used	Optimum Conditions	% Removal	References
1	Methyl orange dye	10 ppm, pH 6.2, 0.4 g TiO_2	72.53%	[119]
2	Rhodamine B	120 min irradiation	78.90%	[104]
3	Rhodamine B (RhB)	10 mg/L dye, 80 min irradiation	90%	[120]
4	Reactive Orange-4 (RO-4) dye	pH 3.5, 180 min irradiation, 25 mg TiO_2	91.19%	[86]
5	Remazol red dye	60 min irradiation, the adsorption capacities of anatase TiO_2 was 0.02 mmol/g	65%	[121]

6	Methylene blue (MB) dye	200 mg TiO_2, initial dye concentration 5 ppm, pH 9, 120 min irradiation	72.86%	[122]
7	Methyl orange dye	20 mg TiO_2 and 120 min irradiation	82%	[123]
8	Methylene blue dye	10 ppm dye, 50 mg TiO_2, pH 10, 6 h exposure to sunlight	98.5%	[124]
9	Acid Blue 113	50 ppm dye, 2 g/L TiO_2, 4 pH and 80 min irradiation	94.43%	**Present study**

3.3.8 Kinetic Study

The kinetics of the photodegradation were conducted concerning time. As the reaction progressed aliquots of the sample were withdrawn at regular time intervals and the absorbance was measured in a UV-visible spectrophotometer. The rate constant for the reaction was determined from the kinetic plot by drawing $\ln \frac{C_0}{C_t}$ vs time (**Fig. 11**) and the reaction was found to follow pseudo-first-order kinetics.

$$\ln \frac{C_0}{C_t} = kt \quad (3)$$

where,

C_0 = Initial dye concentration of AB113 dye,

C_t = Final dye concentration of AB113 dye,

k = Rate constant for the reaction.

From the slope of $\ln \frac{C_0}{C_t}$ vs time graph, the value of the specific reaction rate constant of photocatalytic oxidation of AB 113 was k = 0.03362 min^{-1}.

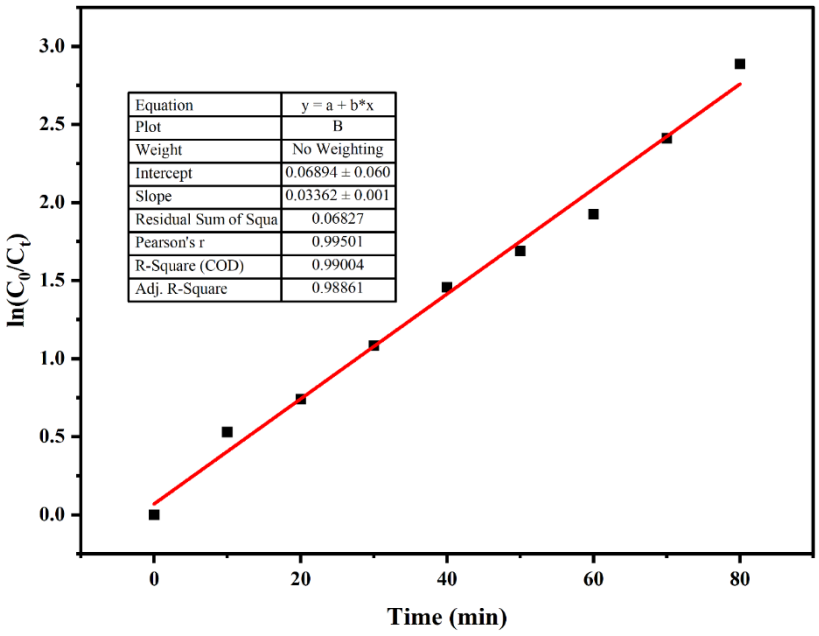

Fig. 3. 11 A linear fitted plot between ln $\frac{C_0}{C_t}$ and time for the computation of specific reaction rate constant.

3.3.9 Antimicrobial activity

Green synthesized nanoparticles mostly exhibited antimicrobial activity. The antimicrobial study was based on the agar well-diffusion method against *Escherichia coli*. The growth of *E. coli* was diminished at well-defined wells with various amounts of TiO_2. The concentration-dependent zone of inhibition was assessed and expressed in millimeters (mm). A maximum of 26.5 ± 0.79 mm diameter inhibition region was exhibited by the TiO_2 concentration of 500 µg/mL (**Fig. 12b**). The antimicrobial activity exhibited by TiO_2 is due to its small size, having enough active specific surface area, cell wall structure of bacterial species, the thickness of membrane cell wall, the formation of Ti^{4+} ions from TiO_2 and the generation of ROS as well as H_2O_2. Proteins, lipids, and lipopolysaccharides make up the outer membrane layer of cells of gram-negative bacteria. The above fact signified that TiO_2 nanoparticles easily penetrated the bacterial cell wall and killed harmful microorganisms quickly [125]. An extensive range of bacterial strains is strongly inhibited by nanomaterials. The metal oxides transfer a positive

charge, whilst the microbes hold a negative charge. Thus, electrochemical interactions between microbes and metal oxides cause oxidation, which in turn causes microbial death. The present finding showed that the green synthesized TiO_2 NPs had high antibacterial activity against the Gram-negative bacteria (*E. coli*) [126]. The bacterial growth rate declined (OD_{600}) as the TiO_2 amount continuously increased (**Fig. 12a**).

It was once thought that the positively charged ions released by TiO_2 NPs and their adhesion to the negatively charged thiol group (-SH) of the proteins on the cytoplasmic membrane served as the germicidal mechanism [127]. As the reaction continues, the cell wall becomes more permeable, which causes the morphology of cellular elements including DNA, ribosomes, and cellular enzymes to change. Eventually, this causes the microorganism to die [128]. Additionally, the microbial cells may become inactive as a result of the photocatalytic activity of TiO_2 NPs by interfering with ion transport and obstructing the metabolic route. This result suggests that TiO_2 NPs synthesized using plant extract can be used as a potential antimicrobial agent to combat bacterial infections and reduce the bacterial load in contaminated water.

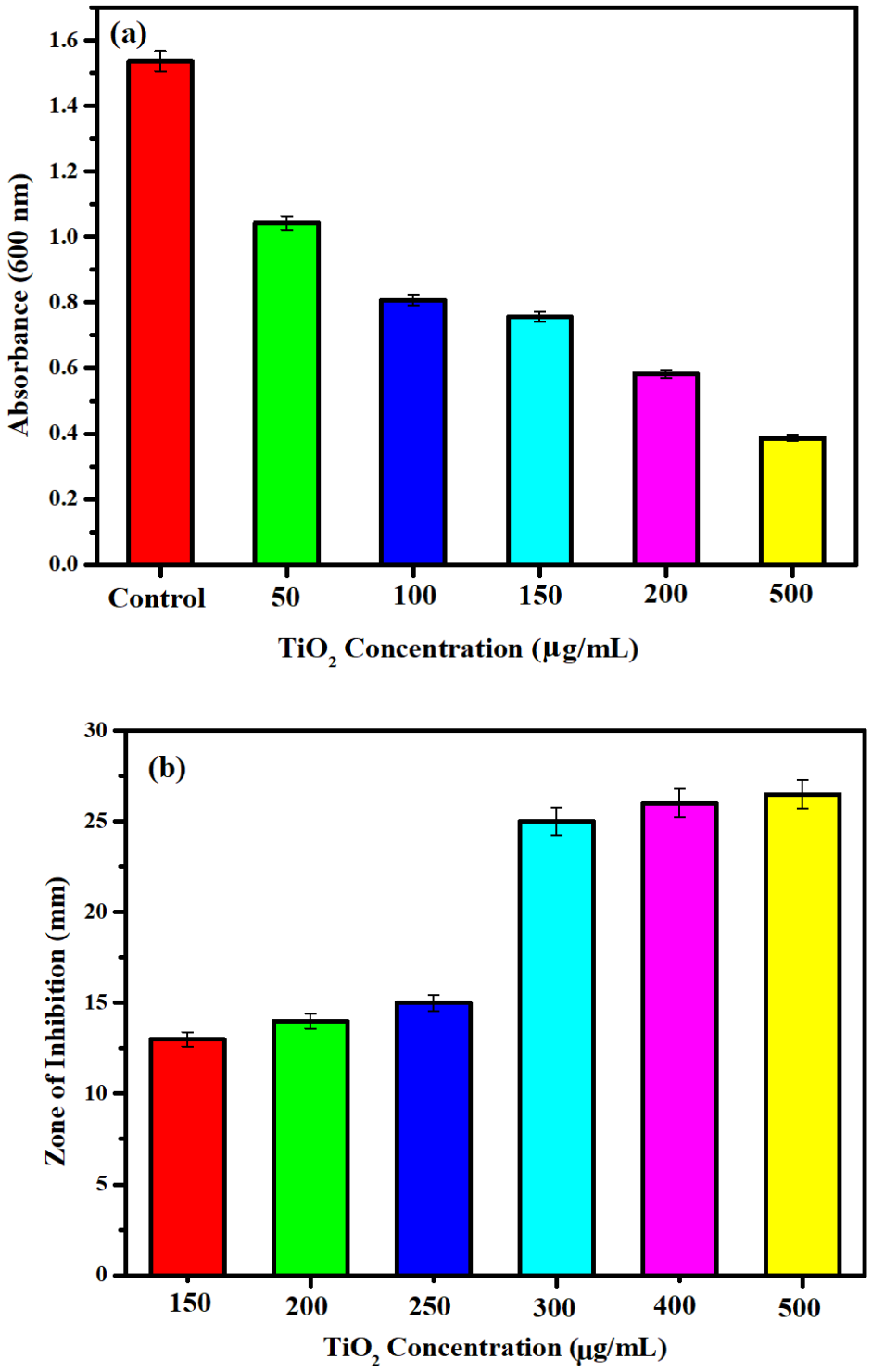

Fig. 3. 12 (a) *E. Coli* growth assessment at various amounts of TiO_2 under ambient conditions Temperature = 30 ± 5°C; bacterial cell concentration 2×10^6 CFU/mL; (b) A typical illustration of the zone of inhibition exhibited by *E. Coli* at various amounts of TiO_2 after 24 h incubation (Temperature = 30 ± 5°C; Error bars depict the standard deviation of the triplicate study).

3.4 Conclusions

Photocatalytic oxidation of various emanating textile dyes using green synthesized TiO_2 NPs emerging as an effective treatment technique. The present findings utilize naturally available *Tinospora cordifolia* plant extract for the synthesis of TiO_2. XRD, SEM, FTIR, and UV–Vis spectroscopy were used to investigate the structural, surface topography, presence of corresponding functional groups and optical characterization of green synthesized TiO_2 NPs, proving their effective fabrication. The green synthesized TiO_2 NPs had an average crystalline size of 15.02 nm, a band gap of 3.13 eV, and an irregular shape. That indicates green synthesized TiO_2 has nano-sized particles with a lower band gap energy than commercially available TiO_2 (3.2 eV). Green synthesized TiO2 NPs demonstrated excellent photocatalytic activity against the oxidation of complex AB 113. A maximum dye removal efficiency of 94.43% was obtained under optimal conditions. The heterogeneous photocatalytic kinetics was linearly fitted against first-order kinetics and obtained the specific reaction rate constant of 0.03362 min^{-1}. Finally, the characteristic antibacterial activity study was also carried out and the outcomes support the typical antibacterial activity against *E. coli.* Therefore, the present study elucidated the enhanced photocatalytic activity and excellent antibacterial activity of green synthesized TiO_2 NPs. Green synthesis must be considered an innovative approach for metal oxide synthesis.